ISSN 0018-151X, High Temperature, 2019, Vol. 57, No. 6, pp. 859–862. © Pleiades Publishing, Ltd., 2019.
Russian Text © The Author(s), 2019, published in Teplofizika Vysokikh Temperatur, 2019, Vol. 57, No. 6, pp. 882–885.

THERMOPHYSICAL PROPERTIES OF MATERIALS

Formation of an Absorbing Layer and Superfast Gallium Arsenide Transition in the Metal State under the Action of Femtosecond Laser Pulses

S. I. Ashitkov[a], A. V. Ovchinnikov[a], *, D. S. Sitnikov[a], and M. B. Agranat[a]

[a]*Joint Institute for High Temperatures, Russian Academy of Sciences, Moscow, 125412 Russia*

**e-mail: a.ovtch@gmail.com*

Received February 26, 2019; revised March 19, 2019; accepted March 27, 2019

Abstract—It has been shown experimentally that an electron-hole plasma forms in the surface layer at a depth of ~30 nm, followed by a transition to the metallic state, when GaAs is exposed to femtosecond laser pulses with an intensity close to the melting threshold. This phenomenon is observed when laser pulses with photon energies are both smaller and larger than the band gap. The formation of an electron-hole plasma and an absorbing layer with metallic properties is mainly due to the mechanism of avalanche ionization by electron impact.

DOI: 10.1134/S0018151X19060038

INTRODUCTION

An important issue in the study of melting and ablation of the surface layer of semiconductors exposed to femtosecond laser pulses is the mechanism of the absorption of laser radiation. For example, in [1–8], similar studies have been carried out under the influence of femtosecond pulses with photon energy of radiation exceeding the band gap E_g. It was assumed [4] that the main part of the laser pulse energy in silicon is absorbed at high intensities as a result of interband, two-photon absorption.

The melting F_{melt} and ablation F_{abl} thresholds for GaAs were measured upon exposure to a pump femtosecond pulse of a chromium-doped forsterite laser at the fundamental wavelength ($\lambda = 1240$ nm) when $\hbar\omega < E_g$, as well as at the second harmonic wavelength when $(2\hbar\omega) > E_g$ and the mean free path of a photon is several orders of magnitude smaller than at the main wavelength [9]. Despite the large difference in the length of photon path, the threshold energy densities of the heating femtosecond pulse at two wavelengths are practically the same.

This paper presents the results of experimental studies of the complex dielectric permittivity of GaAs at wavelengths with a photon energy greater and less than the band gap for fluence of the heating pulse near the melting and ablation thresholds of the surface layer. The dependence of the absorption depth on the intensity of the femtosecond pulses was obtained based on the measurement results. The mechanism of the formation of a dense electron-hole plasma, which leads to the formation of a thin, strongly absorbing surface layer, is discussed. When the melting threshold is significantly exceeded ($0.9F_{abl}$) at subpicosecond times, the transition of the semiconductor to the metallic state, in which the real part of the dielectric constant becomes negative, was observed.

EXPERIMENTAL

The radiation source was a unique chromium-doped forsterite laser system that allows the generation of femtosecond pulses with a wavelength $\lambda = 1240$ nm [10]. The pulse duration (FWHM), which was measured with an autocorrelator, was $\tau \approx 100$ fs in the sech^2 envelope approximation. The time profile of the pulse was also measured in a wide range of intensity changes with a third-order cross-correlator. The ratio of intensity (contrast) at the maximum to the intensity for 1 ps to the maximum was at least 10^4; for 2 ps, it was more than 10^6.

The method to measure the threshold values of the fluence of a heating pulse during melting F_{melt} and ablation F_{abl} of the semiconductor surface layer has been described in detail [9]. Table 1 presents the measurements of the threshold values of the fluence on the sample surface at an incidence angle of 45° *p*-polarized heating pulse at wavelengths of 1240 nm and 620 nm for GaAs.

The experiments were carried out with a 0.4-mm-thick, polished, single-crystal (100) GaAs sample.

Table 1. GaAs melting and ablation thresholds [9]

Material	Wavelength, nm	F_{melt}, mJ/cm^2	F_{abl}, mJ/cm^2
GaAs	620	90	190
	1240	130	200

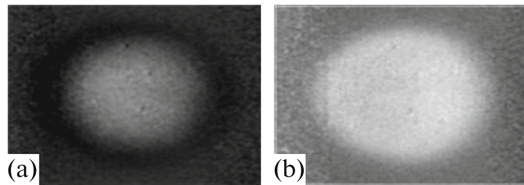

Fig. 1. Spatial distribution of the amplitude (a) and phase (b) of the complex reflection coefficient at an energy density in the center of the spot of $1.1F_{\text{abl}}$.

After each exposure to a heating pulse, the sample was displaced to a new place.

Femtosecond interference microscopy was used to study the change in the optical properties of the sample in the affected area [11, 12]. This makes it possible to obtain information on the dynamics of changes in the amplitude and phase of the reflected wave of the probe radiation with a time resolution of $\sim 10^{-13}$ s in the pump–probe measurement scheme. The surface of the semiconductor was heated by radiation at a fundamental wavelength of 1240 nm, and the radiation was used as a probe pulse at wavelengths of $\lambda = 1240$ nm and at $\lambda = 620$ nm of the second harmonic. The use of Fourier processing of the interferograms and a CCD camera with a matrix size of 1024 × 1024 pixels and a resolution of 12 bits allows these parameters of the optical scheme of the interferometer [12] to realize the accuracy in the measurement of a change in the reflection coefficient modulus of less than 1% and a phase change of $\sim\pi/200$ for a spatial resolution of ~2 microns. At a wavelength of 1240 nm, the CCD camera worked in the two-photon absorption mode.

The dependence of the change in the amplitude and phase of the reflection coefficient on the fluence of the heating pulse was measured in a single pulse via comparison with the measured Gaussian distribution of the fluence over the beam cross section [12]. The relative error of fluence measurements is ±10%.

Figure 1 shows the characteristic spatial distributions of the amplitude and phase of the complex reflection coefficient of the probe pulse ($\lambda = 620$ nm) from the surface of gallium arsenide at a fluence of the heating pulse ($\lambda = 1240$ nm) that is greater than the ablation threshold F_{abl}. The experiments were carried out with a fixed delay (~200 fs) of the probe pulse, i.e., almost immediately after the end of the heating pulse.

Figure 2 shows the changes in the amplitude and phase of the reflection coefficient of the probe pulse at wavelengths of 620 and 1240 nm on the fluence of the heating pulse immediately after its action.

Fresnel formulas are used to determine the optical constants from the measured values of the amplitude and phase of the complex reflection coefficient. The use of Fresnel formulas is valid in the presence of a sharp boundary and uniformity of dielectric permittivity along the depth of the probed layer. When the probing occurs with a time delay of 200 fs relative to the beginning of a heating laser pulse, the motion of the surface-layer boundary is insignificant, and therefore the boundary can be considered sharp, but the carrier concentration in the probed layer is inhomogeneous. Nevertheless, since the purpose of the experiments is to study the change in the optical constants from the energy flux of the heating pulse, not to measure their absolute values, the authors believe that it is possible to use Fresnel formulas similar to [13, 14].

Figure 3 shows the imaginary k and real n parts of the complex refractive index of the surface layer of gallium arsenide as calculated by the Fresnel formulas similarly to [12, 14] for two wavelengths of the probe pulse (620 and 1240 nm) from the energy flux of the heating laser pulse.

Table 2 gives the values of the optical constants for the sample of unirradiated gallium arsenide.

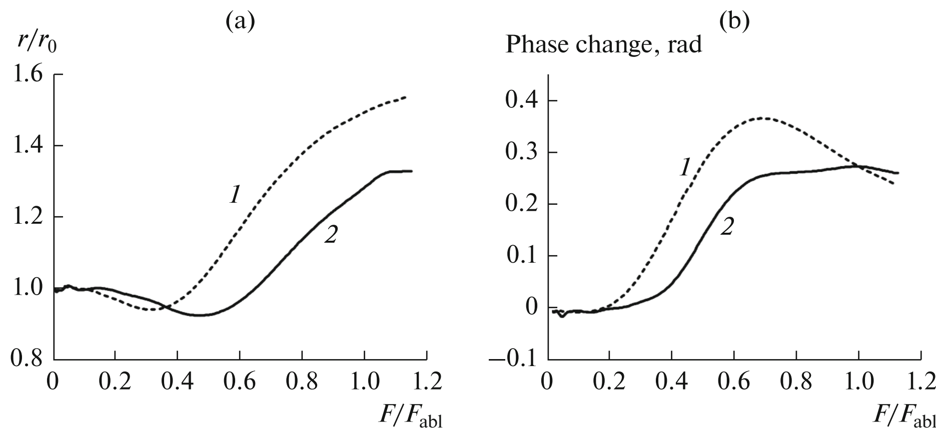

Fig. 2. Dependence of the amplitude (a) and phase (b) of the GaAs complex reflection coefficient on the energy density of the heating laser pulse at two wavelengths of probe radiation: (*1*) 1240 nm, (*2*) 620.

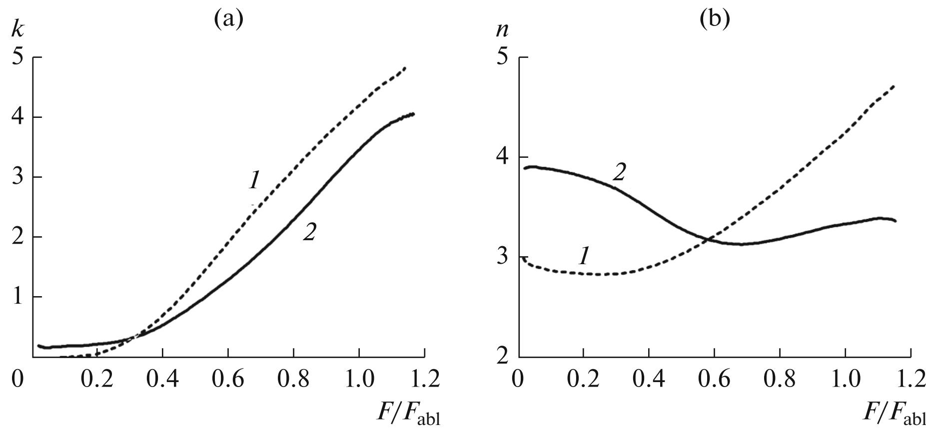

Fig. 3. Depending on the energy flux of the heating laser pulse of the imaginary (a) and real (b) parts of the complex refractive index of the surface layer of gallium arsenide: (*1*, *2*) as in Fig. 2.

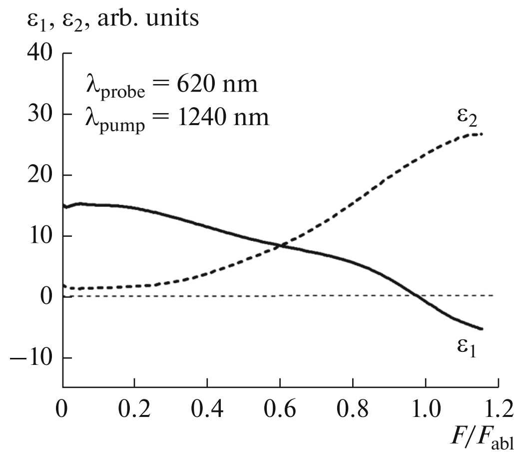

Fig. 4. Dependence of the real and imaginary parts of the dielectric constant of GaAs on the energy density at a wavelength of probing radiation of 620 nm.

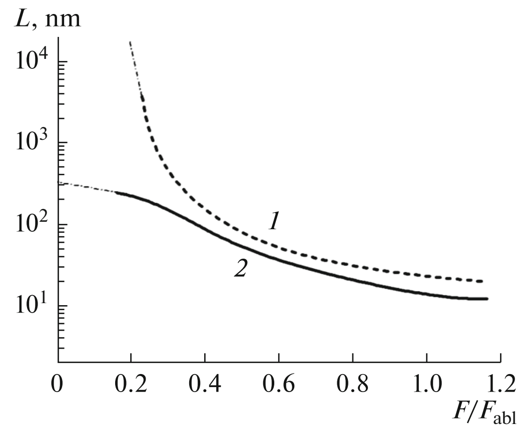

Fig. 5. Dependence of changes in the absorption depth of gallium arsenide on the energy density of a heating laser pulse at two wavelengths: (*1*) 1240 nm, (*2*) 620; dash-dotted line—approximation of *L* for an unexcited sample.

Figure 4 presents the dependences of the real and imaginary parts of the dielectric constant on the fluence for gallium arsenide immediately after the end of the heating pulse.

It can be seen that the real part of the dielectric constant becomes negative, i.e. a semiconductor–metal transition occurs, at a fluence of the heating pulse of $0.9F_{abl}$.

Based on the results, it is possible to evaluate the manner in which the depth of the surface absorbing layer changes l ($l = \lambda/(4\pi k)$) depending on the fluence of the heating pulse at various wavelengths, when the photon energy of the radiation is greater (at 620 nm) or less (1240 nm) than that of the band gap. Figure 5 shows the obtained dependences.

Analysis of the experimental data shows that the absorption depths at different wavelengths practically coincide for the fluence above $0.4F_{abl}$, although the absorption depth in the unexcited state differs by four orders of magnitude and is less than 1 μm at a wavelength of 620 nm and about 1 cm at 1240 nm. When the fluence of the heating pulse is close to the ablation threshold, the absorbing layer "collapses" to values of ~30–40 nm as a result of the transition of the semiconductor to the metallic state.

Thus, the absorption mechanism in GaAs at high radiation intensities is similar to the breakdown mechanism of transparent dielectrics [16]. In this

Table 2. Real and imaginary parts of the GaAs complex refractive index for wavelengths of 620 and 1240 nm [15]

Wavelength nm	*n*	*k*
1240	3.232	1.33×10^{-4}
620	3.87	0.2

case, the damage threshold weakly depends on the photon energy of the heating laser. Qualitatively, the absorption mechanism can be represented as follows (similar to [16]).

Seed electrons in the conduction band, which arise, for example, due to two (or more) photon processes and absorb the energy of laser radiation by interacting with phonons (intraband absorption). As a result of the absorption, there are electrons with an energy ε greater than the band gap $\varepsilon > E_g$. Such electrons are capable of generating electron-hole pairs via impact ionization, leading to an increase in the electron concentration in the conduction band to values corresponding to the transition to the metallic state.

CONCLUSIONS

The studies obtained the dependences of the absorption depth of radiation with a photon energy greater than or less than the band gap in the surface layer of gallium arsenide on the energy density of the femtosecond laser pulses of the visible and near infrared spectral ranges near the melting and ablation thresholds. The obtained dependences show that the absorption-depth values at different wavelengths practically coincide at different wavelengths when the fluence of the heating pulse is below the melting threshold ($0.5F_{melt}$). The obtained data allow us to explain the equality of thresholds [9] in the case of exposure to radiation with a photon energy greater or less than the band gap.

ACKNOWLEDGMENTS

All of the experimental work was performed on a unique terawatt chrome-forsterite laser system at the Laser Femtosecond Complex Center for Collective Use, Joint Institute for High Temperatures, Russian Academy of Sciences.

REFERENCES

1. Shank, C.V., Yen, R., and Hirlimann, C., *Phys. Rev. Lett.*, 1983, vol. 50, p. 454.
2. Tanaka, T., Harata, A., and Sawada, T., *J. Appl. Phys.*, 1997, vol. 82, p. 4033.
3. Sokolowski-Tinten, K., Bialkowski, J., Boring, M., Cavalleri, A., and von der Linde, D., *Phys. Rev. B: Condens. Matter Mater. Phys.*, 1998, vol. 58, p. R11805.
4. Sokolowski-Tinten, K. and von der Linde, D., *Phys. Rev. B: Condens. Matter Mater. Phys.*, 2000, vol. 61, p. 2643.
5. Callan, J., Kim, A.M.-T., Huang, L., and Mazur, E., *Chem. Phys.*, 2000, vol. 251, p. 167.
6. Bonse, J., Brzezinka, K.-W., and Meixner, A.J., *Appl. Surf. Sci.*, 2004, vol. 221, p. 215.
7. Ionin, A.A., Kudryashov, S.I., Seleznev, L.V., and Sinitsyn, D.V., *JETP Lett.*, 2011, vol. 94, p. 34.
8. Gunnella, R., Zgrablic, G., Giangrisostomi, E., D'Amico, F., Principi, E., Masciovecchio, C., Di Cicco, A., and Parmigiani, F., *Phys. Rev. B*, 2016, vol. 94, 155427.
9. Agranat, M.B., Anisimov, S.I., Ashitkov, S.I., Ovchinnikov, A.V., Kondratenko, P.S., Sitnikov, D.S., and Fortov, V.E., *JETP Lett.*, 2006, vol. 83, no. 11, p. 501.
10. Agranat, M.B., Ashitkov, S.I., Ivanov, A.A., Konyashchenko, A.V., Ovchinnikov, A.V., and Fortov, V.E., *Quantum Electron.*, 2004, vol. 34, p. 506.
11. Temnov, V.V., Sokolowski-Tinten, K., Zhou, P., and von der Linde, D., *J. Opt. Soc. Am. B*, 2006, vol. 23, p. 1954.
12. Sitnikov, D.S., Komarov, P.S., Ovchinnikov, A.V., and Ashitkov, S.I., *Tech. Phys.*, 2009, vol. 54, no. 4, p. 520.
13. Morikami, H., Yoneda, H., Ueda, K., and More, R.M., *Phys. Rev. E: Stat., Nonlinear, Soft Matter Phys.*, 2004, vol. 70, 035401.
14. Ashitkov, S.I., Komarov, P.S., Struleva, E.V., Yurkevich, A.A., and Agranat, M.B., *High Temp.*, 2016, vol. 54, no. 6, p. 899.
15. Palik, E.D., *Handbook of Optical Constants of Solids II*, San Diego: Academic, 1991.
16. Schaffer, C.B., Brodeur, A., and Mazur, E., *Measurement Sci. Technol.*, 2001, vol. 12, no. 11, p. 1784.